Optical Materials 141 (2023) 113948

Contents lists available at ScienceDirect

Optical Materials

journal homepage: www.elsevier.com/locate/optmat

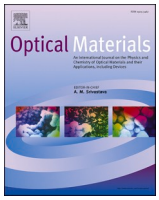

Research Article

TSL, OSL and scintillation properties of Tb-doped barium fluoride translucent ceramics

Naoki Kawano [a,*], Takumi Kato [b], Daisuke Nakauchi [b], Yuma Takebuchi [b], Hiroyuki Fukushima [b], Daiki Shiratori [b], Luiz G. Jacobsohn [c], Takayuki Yanagida [b]

[a] Graduate School of Engineering Science, Akita University, 1-1Tegata Gakuen-machi, Akita, 010-8502, Japan
[b] Graduate School of Science and Technology, Nara Institute of Science and Technology, 8916-5 Takayama-cho, Ikoma, Nara, 630-0192, Japan
[c] Department of Materials Science and Engineering, Clemson University, 515 Calhoun Dr, Clemson, SC, 29634, USA

ARTICLE INFO

Keywords:
Tb^{3+} ion
Barium fluoride
Translucent ceramic
Dosimeter

ABSTRACT

We report on the fabrication of Tb-doped barium fluoride translucent ceramics, and their scintillation and dosimetric characteristics. The Tb-doped barium fluoride ceramics were fabricated by spark plasma sintering. Scintillation derived from the 4f→4f transitions of Tb^{3+} under X-rays was observed from the Tb-doped barium fluoride ceramics. Their decay times under X-rays were about 10 ms. Further, thermally-stimulated luminescence originating from the transitions was detected, and their dose responses were observed in the range of 0.1–100 mGy. Moreover, the Tb-doped barium fluoride ceramics exhibited optically-stimulated luminescence (OSL), and three exponential decay components were detected in the OSL decay curves.

1. Introduction

Luminescent materials for ionizing radiation detection and measurements have been playing a significant role in a wide variety of industrial fields, and they can be divided into storage phosphors and scintillators [1,2]. Specifically, dosimeters based on storage phosphors have been employed with the aim to determine radiation doses for environmental and personal monitoring [3]. When a phosphor is exposed to ionizing radiation, free charge carriers such as electrons and holes are formed, and some of them are captured at defects in a metastable state. After external stimulation (e.g., heat, light), the charge carriers are released from the metastable state, possibly followed by emission due to electron-hole recombination at a luminescence center. The emissions are known as optically-stimulated luminescence (OSL) or thermally-stimulated luminescence (TSL) when the phosphors are stimulated by a photon or thermal energy, respectively [4,5]. On the other hand, scintillators can emit photons immediately when exposed to ionizing radiation, and they have been employed for various applications such as natural resources exploration, medical diagnosis, and security inspection [6–9]. To date, various kinds of luminescent materials (e.g., sintered ceramics, glasses, single crystals, and nanomaterials) have been developed for ionizing radiation measurements [10–16].

Transparent ceramics have gained increasing attention in the ionizing radiation detection community. While single crystals have been mostly considered because of their high light yield, transparent ceramics can be fabricated at lower cost and achieve uniform doping and high luminosity [17–25]. For example, a cerium-doped gadolinium garnet (GYGAG:Ce) scintillator achieved a high light yield of about 50000 photons/MeV, and energy resolution of approximately 5% at 662 keV [26]. In addition to this garnet ceramic, some transparent oxide ceramics such as $Y_3Al_5O_{12}$:Ce, Lu_2O_3:Eu, $Lu_3Al_5O_{12}$:Ce have been fabricated for scintillation applications [27–29]. Further, our group has fabricated several transparent fluoride ceramics by spark plasma sintering (SPS) [30–33]. For instance, a calcium fluoride transparent ceramic doped with Eu showed scintillation with a light yield of about 17000 photons/MeV originating from the 5d→4f transition of Eu^{2+} [30]. In that ceramic, TSL was also observed within the X-ray dose range 0.1–1000 mGy. Moreover, other fluorides like strontium fluoride and magnesium fluoride transparent ceramics were also fabricated for radiation detection [30–34].

In this work, we focused on barium fluoride transparent ceramics. Barium fluoride is a well-known material for ionizing radiation measurements since it shows a large effective atomic number (52.7) that is advantageous for the detection of high energy photons (e.g., gamma-ray and X-rays) [35,36]. To date, scintillation and dosimetric properties of several barium fluoride single crystals doped with rare-earth ions have

* Corresponding author.
E-mail address: n-kawano@gipc.akita-u.ac.jp (N. Kawano).

https://doi.org/10.1016/j.optmat.2023.113948
Received 6 January 2023; Received in revised form 12 April 2023; Accepted 23 May 2023
Available online 28 May 2023

been evaluated. For instance, a barium fluoride single crystal doped with Ce^{3+} showed TSL with a glow peak at 416 K, and the activation energy was estimated to be about 0.83 eV [37]. Further, the crystal showed scintillation at around 320 nm with two major decay times of 47 and 260 ns, and its light yield was 1210 photoelectron yield/MeV. Furthermore, we have fabricated undoped barium fluoride transparent ceramics synthesized by SPS for ionizing radiation measurements [35]. The undoped barium fluoride transparent ceramic exhibited a broad emission due to self-trapped excitons (STEs) when excited by X-rays, and its scintillation light yield was 6000 photons/MeV. Further, the scintillation properties of barium fluoride transparent ceramics with Ce^{3+} were reported by J. Luo et al., and the light yield was approximately 5100 photons/MeV, which was comparable to that of the single crystal counterpart [38]. In this work, barium fluoride ceramics doped with Tb were synthesized by SPS and their scintillation and dosimetric properties are reported. The underpinning goal is to achieve a more intense signal from the efficient $^5D_4 \rightarrow {}^7F_5$ transition of the Tb^{3+} ions than from the intrinsic emission of the host. This will naturally promote higher detection efficiency of ionizing radiation combined with better spectral matching with the quantum efficiency of photomultiplier tubes [39–41]. These features are particularly relevant for imaging plate applications [42–44].

2. Experimental methods

The Tb-doped barium fluoride translucent ceramics were fabricated as follows. TbF_3 and BaF_2 in specific molar ratios (0.1, 0.5, and 1 M %) were mixed, placed into a graphite die and held between two punches. Further, they were heated to 720 °C at a 10 °C/min rate, and kept for 10 min under 10 MPa in a furnace (Sinter Land LabX-100). Subsequently, the temperature was increased to 960 °C at a 10 °C/min rate, and kept under 100 MPa for 15 min. Finally, the temperature decreased to 200 °C at a 65 °C/min under 6 MPa. After the fabrication of the Tb-doped barium fluoride ceramics, they were polished with a polisher (IM-P2, IMT). The obtained barium fluoride ceramics had thickness of about 1.0 mm.

X-ray diffraction patterns were recorded with a RINT-2200V diffractometer (Rigaku). In-line optical transmittance spectra were obtained using a V-750 spectrometer (JASCO). Scintillation spectra under X-ray irradiation were recorded with our home-made detection system [45]. Further, afterglow and scintillation decay curves under pulsed X-ray irradiation were recorded with our system [46]. For the evaluation of dosimetric properties, TSL glow curves were recorded at a temperature rate of 1 °C/s using a TL-2000 spectrometer (Nanogray) whose measurable wavelength range was from 300 nm to 550 nm. TSL spectra were measured using a ceramic heater, a SCRSHQ-A temperature controller (Sakaguchi), and a QEPro spectrometer (Ocean Optics). TSL glow curves were not corrected for the thermal quenching of the luminescence centers. In addition, OSL spectra and OSL decay curves were recorded using a FP-8600 spectrometer (JASCO). The OSL spectra were recorded in the range of 300–500 nm under 560 nm stimulation light, and the OSL decay curve was obtained by monitoring at 380 nm.

3. Results and discussion

A photograph of the Tb-doped barium fluoride ceramics is exhibited in Fig. 1. These barium fluoride ceramics were found to be translucent with the printed lines behind the Tb-doped barium fluoride ceramics being visible through them. Fig. 2 shows the in-line transmittance spectra of the Tb-doped barium fluoride ceramics. Their transmittances at 650 nm were 32% (0.1% Tb), 37% (0.5% Tb), 28% (1% Tb). No absorption bands derived from the 4f→4f transitions of Tb^{3+} were detected. Furthermore, no clear change of the optical transmittance was observed as a function of the TbF_3 content. On the other hand, optical transparency was affected by the specific fabrication conditions, including the incorporation of carbon from the graphite dies and punches.

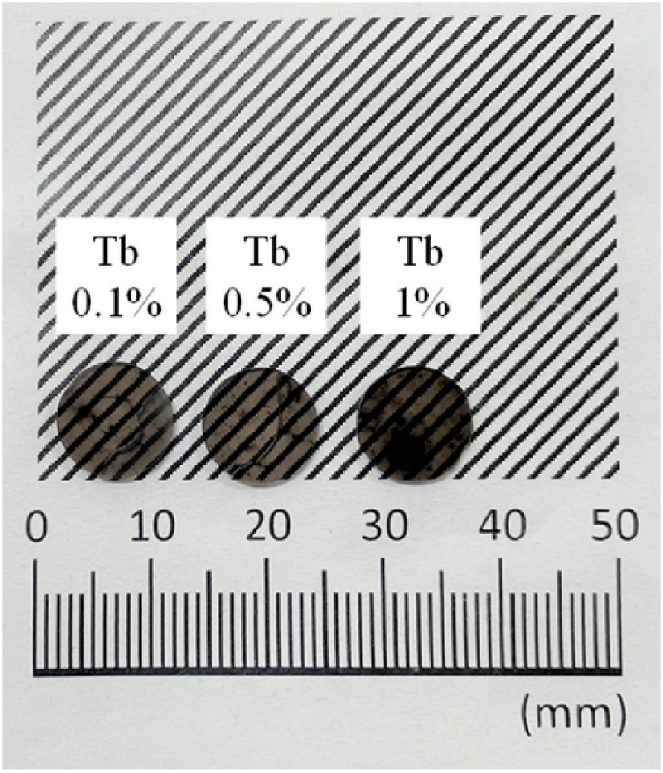

Fig. 1. Visual appearance of the Tb-doped barium fluoride translucent ceramics.

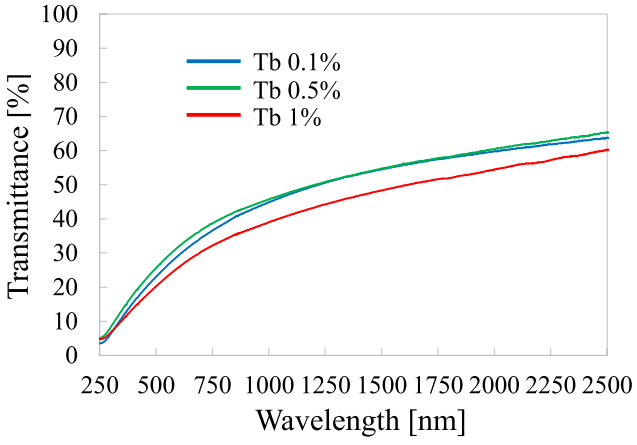

Fig. 2. Transmittance spectra of the Tb-doped barium fluoride translucent ceramics.

Fig. 3 exhibits the X-ray diffraction patterns of the Tb-doped barium fluoride ceramics. A series of diffraction peaks appeared in the 20–80° range. These peaks were identified in reference to the pattern of undoped barium fluoride (No: 01-088-2466). No impurity phase was detected in these ceramics.

Fig. 4 (a) shows the scintillation spectra of the Tb-doped barium fluoride ceramics, and the enlarged scintillation spectra ranging within 200–370 nm are exhibited in Fig. 4(b). Sharp peaks centered at 380, 416, 433, 477 540, 587, and 623 nm were observed from the Tb-doped barium fluoride ceramics. They were ascribed to the 4f→4f transitions of Tb^{3+}, indicating that Tb^{3+} ions were doped into the barium fluoride ceramics [39,47–49]. Further, a weak broad peak appeared at around 325 nm, and this weak peak was attributed to STEs in a barium fluoride

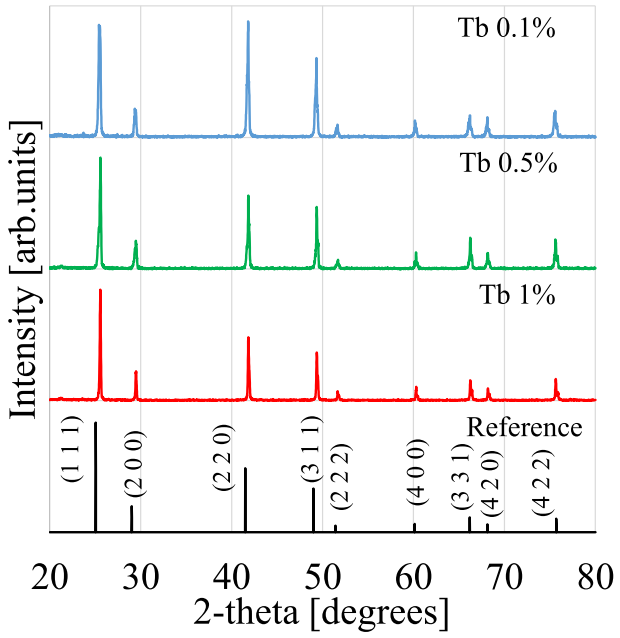

Fig. 3. X-ray diffraction patterns of the Tb-doped barium fluoride translucent ceramics together with PDF file no. 01-088-2466.

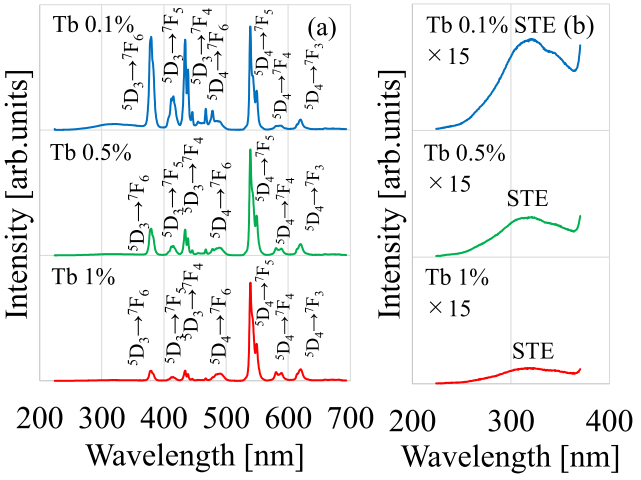

Fig. 4. (a) X-ray induced scintillation spectra of the Tb-doped barium fluoride translucent ceramics and (b) enlarged spectra in the 200–370 nm range highlighting STE emission.

host [35]. Its STE intensity decreased for higher concentrations of Tb.

Scintillation decay curves of the Tb-doped barium fluoride ceramics are exhibited in Fig. 5. The curves were approximated by a single exponential decay function. The lifetimes derived through this analysis were 12.6 ms (0.1% Tb), 8.2 ms (0.5% Tb), 8.1 ms (1% Tb). These times were compatible to the 4f→4f transitions of Tb^{3+} as per previous studies [39,47,48]. The lifetimes decreased with increasing the TbF_3 concentration, possibly due to concentration quenching.

To evaluate dosimetric properties, TSL glow curves of the Tb-doped barium fluoride ceramics were recorded (Fig. 6). The Tb-doped barium fluoride ceramics were previously irradiated with X-rays (100 mGy). As exhibited in Fig. 6, two TSL glow peaks at approximately 60 and 110 °C were observed from the 0.1–0.5% Tb-doped barium fluoride ceramics while the 1% Tb-doped barium fluoride ceramic showed a single peak at approximately 95 °C. The intensity of the 0.1% Tb-doped barium fluoride ceramic was the highest, and the intensity decreased with the TbF_3 concentration. The low peak temperature of the observed TSL glow peaks might lead to TSL fading based on a past study [50].

To investigate the origin of TSL, the TSL spectra of the Tb-doped barium fluoride ceramics were measured at 100 °C (in Fig. 7). Prior to the measurement of the TSL spectra, the Tb-doped barium fluoride ceramics were exposed to X-rays (1 Gy). Emission peaks attributed to the 4f→4f transitions of Tb^{3+} were detected from the Tb-doped barium fluoride ceramics [39,47,48]. The observation of these emission lines indicated that the recombination center of electrons and holes was Tb^{3+} ions in the barium fluoride host. The progressive decrease in intensity of Tb^{3+} for higher Tb concentrations is possibly due to concentration quenching.

Fig. 8 shows the TSL dose response curves of the Tb-doped barium fluoride ceramics. The 0.1–1% Tb-doped barium fluoride ceramics showed a TSL response in the 0.1–100 mGy dose range. The lowest irradiation dose was assumed to be the lowest measurable dose (100 μGy), noting that it was larger than that of conventional TSL dosimeters (e.g., LiF:Mg,Ti; 20 μGy) [3]. It is likely that further improvement in optical transparency of the ceramic host and optimization of the Tb concentration will lower the lowest measurable dose, improving the dosimetric response of this material. The linearity of the dose response was evaluated using the function ($y = a^x + b$). Fitting revealed the x values to be slightly above 1 and $R^2 = 0.99$ indicating these ceramics to have a slight supralinearity against X-ray irradiation.

Further, the OSL characteristics of the Tb-doped barium fluoride ceramics were investigated. Fig. 9 exhibits the OSL spectra under 560 nm stimulation light after X-ray irradiation (10 Gy). Emission peaks appeared at approximately 383, 420, 435, and 488 nm. The emission spectra were similar to those in the scintillation spectra and in past studies; therefore, they were attributable to the 4f→4f transitions of Tb^{3+} [39,47,48]. Interestingly, the OSL spectra are dominated by the UV emission $^5D_3 \rightarrow {}^7F_6$ at 383 nm though this dominance decreased in relative intensity for higher Tb concentrations possibly due to concentration quenching of this emission band. Further, OSL decay curves under 560 nm stimulation light were recorded (Fig. 10). The decay curves could be described by the sum of three exponential decay functions. The obtained time constants of the Tb-doped barium fluoride ceramics decay curves, 11, 41 and 140 s, were essentially unchanged with the Tb concentrations suggesting there were at least three processes associated with OSL mechanism in the Tb-doped barium fluoride ceramics. Further, the observed decay times should not be affected by the afterglow since the afterglow intensity at 50 ms was comparable to the background signal intensity of the Tb-doped barium fluoride ceramics as shown in Fig. 5.

Moreover, the OSL dose response of the Tb-doped barium fluoride ceramics was determined (Fig. 11). The linearity of the OSL response was investigated in the range of 10–10000 mGy for the 0.1–0.5% Tb-doped barium fluoride ceramics and 100–10000 mGy for the 1% Tb-doped barium fluoride ceramic due to its reduced light output. The lowest OSL measurable dose (10 mGy) of the 0.1–0.5% Tb-doped barium fluoride ceramics were higher than that of common OSL materials (e.g., $MgAl_2O_4$: 0.65 mGy [51], Al_2O_3:C: 50 μGy [3], and BaFBr:Eu: 0.1 mGy [52]). In addition, the dose linearity was also evaluated using the function ($y = a^x + b$) with x values fluctuating around unity and $R^2 = 0.99$, indicating linearity of the OSL response.

4. Conclusions

Barium fluoride translucent ceramics with different amounts of TbF_3 were fabricated, and their scintillation and dosimetric characteristics were evaluated. The 4f→4f transitions of Tb^{3+} ions served as the scintillation luminescence centers and also as the TSL and OSL recombination centers. The 0.1% Tb-doped barium fluoride ceramic exhibited the brightest scintillation and the highest TSL and OSL intensities. The

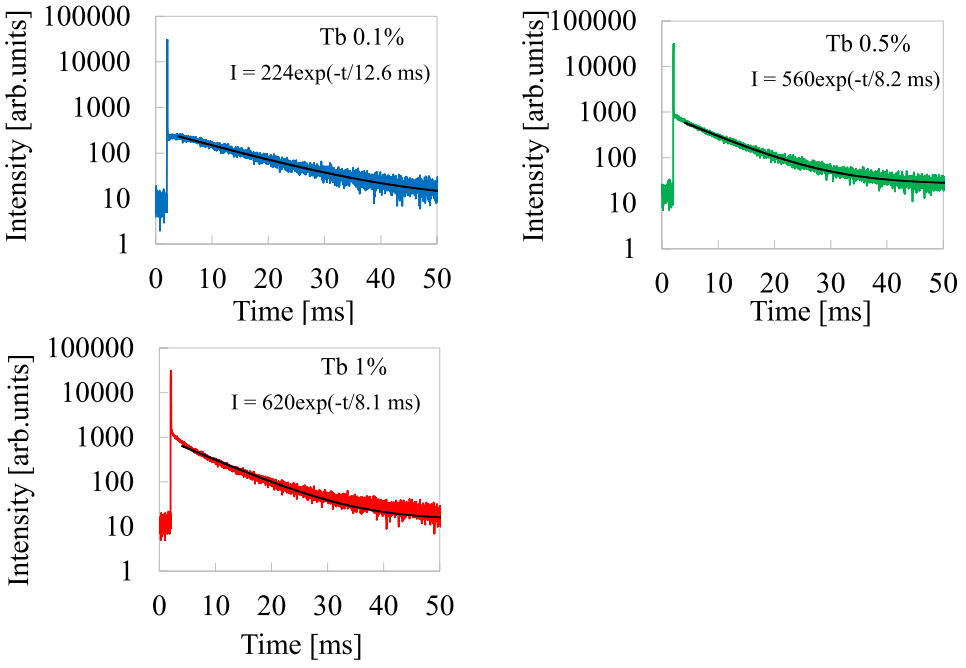

Fig. 5. X-ray induced scintillation decay time profiles of the Tb-doped barium fluoride translucent ceramics together with best-fitting with a single exponential function.

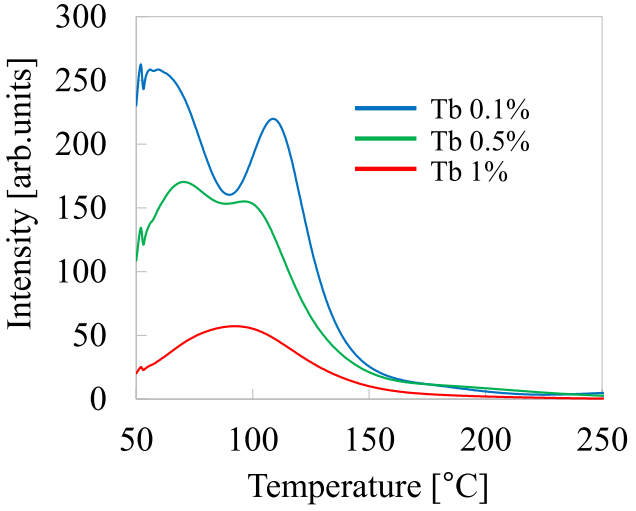

Fig. 6. TSL glow curves of the Tb-doped barium fluoride translucent ceramics.

lowest detectable limits of this ceramic were 0.1 mGy for TSL and 10 mGy for OSL.

CRediT authorship contribution statement

Naoki Kawano: carried out the experiments, conceived the original idea, analyzed the experimental data, wrote the manuscript. **Takumi Kato:** carried out the experiments, conceived the original idea. **Daisuke Nakauchi:** carried out the experiments. **Yuma Takebuchi:** carried out the experiments. **Hiroyuki Fukushima:** carried out the experiments. **Daiki Shiratori:** carried out the experiments. **Luiz G. Jacobsohn:** analyzed the experimental data, revised the manuscript, supported the project as TI-FRIS international mentor. **Takayuki Yanagida:** supervised the project.

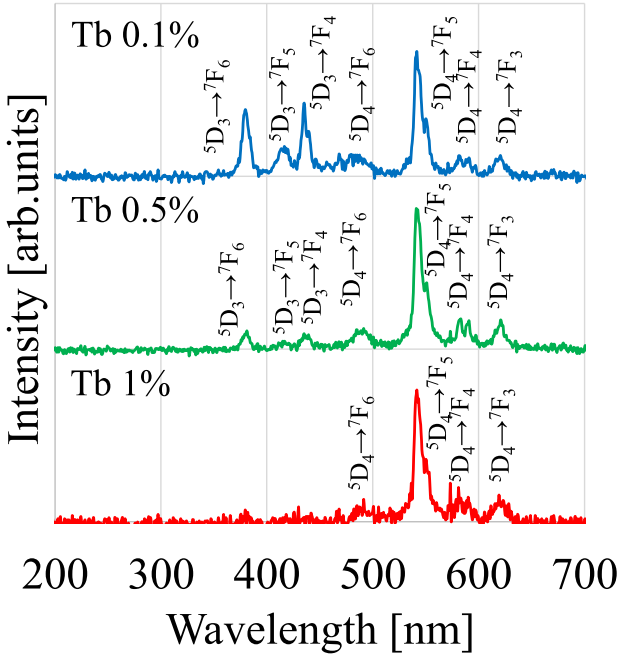

Fig. 7. TSL spectra of the Tb-doped barium fluoride translucent ceramics at 100 °C.

Declaration of competing interest

The authors declare that they have no known competing financial interests or personal relationships that could have appeared to influence the work reported in this paper.

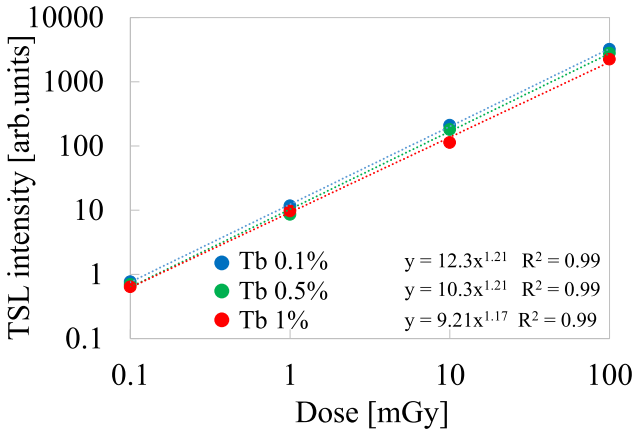

Fig. 8. TSL dose response curves of the Tb-doped barium fluoride translucent ceramics.

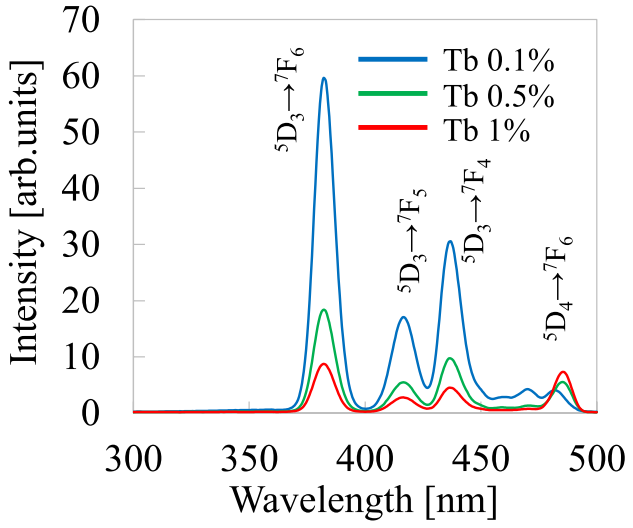

Fig. 9. OSL spectra of the Tb-doped barium fluoride translucent ceramics.

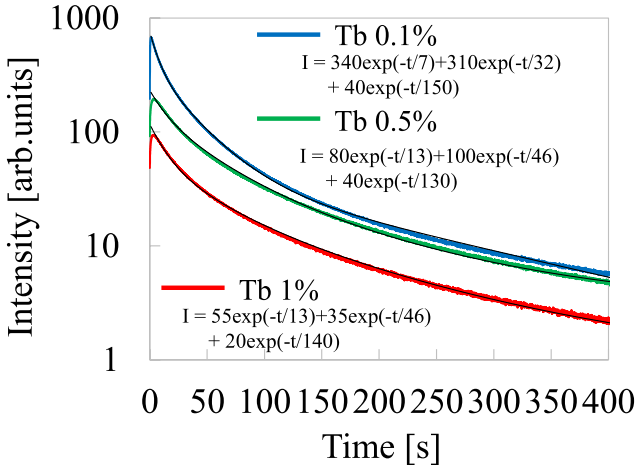

Fig. 10. OSL decay curves of the Tb-doped barium fluoride translucent ceramics together with best fitting with three exponential functions.

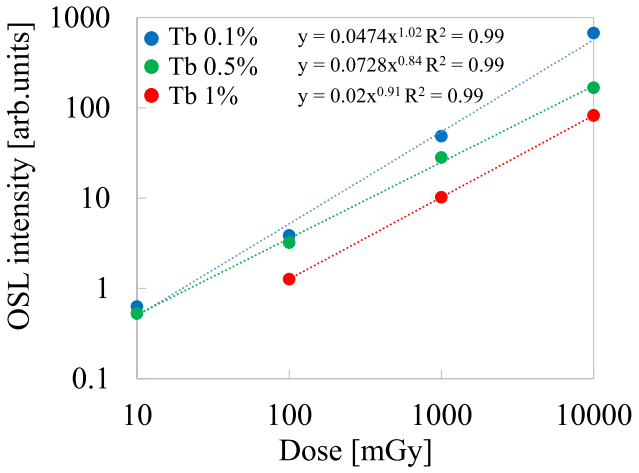

Fig. 11. OSL dose response curves of the Tb-doped barium fluoride translucent ceramics.

Data availability

The authors do not have permission to share data.

Acknowledgement

This work was supported by the Tohoku Initiative for Fostering Global Researchers for Interdisciplinary Sciences (TI-FRIS) of Japan Science and Technology Agency in Japan. L.G. Jacobsohn acknowledges support by the National Science Foundation under Grant No. 1653016 in United States.

References

[1] T. Yanagida, Inorganic scintillating materials and scintillation detectors, Proc. Jon. Acad. Ser. B 94 (2018) 75–97.
[2] T. Yanagida, Ionizing radiation induced emission: scintillation and storage-type luminescence, J. Lumin. 169 (2016) 544–548.
[3] B.C. Bhatt, Thermoluminescence, optically stimulated luminescence and radiophotoluminescence dosimetry: an overall perspective, Radiat. Protect. Environ. 34 (2011) 6–16.
[4] M.R. Mayhugh, R.W. Christy, N.M. Johnson, Thermoluminescence and color center correlations in dosimetry LiF, J. Appl. Phys. 41 (1970) 2968.
[5] S.W.S. McKeever, Optically stimulated luminescence: a brief overview, Radiat. Meas. 46 (2011) 1336–1341.
[6] C.L. Melcher, Scintillators for well logging applications, Nucl. Instrum. Meth. Phys. Res. B 40– 41 (1989) 1214–1218.
[7] C. Ronda, H. Wieczorek, V. Khanin, P. Rodnyi, Review—scintillators for medical imaging: a tutorial overview, ECS J. Solid State Sci. Technol. 5 (1) (2016) R3121–R3125.
[8] J. Glodo, Y. Wang, R. Shawgo, C. Brecher, R.H. Hawrami, J. Tower, K.S. Shah, New developments in scintillators for security applications, Phys. Procedia 90 (2017) 285–290.
[9] S.E. Derenzo, M.J. Weber, E. Bourret-Courchesne, M.K. Klintenberg, The quest for the ideal inorganic scintillator, Nucl. Instrum. Methods Res. Sect. A. 505 (2003) 111–117.
[10] M.J. Cie'slak, K.A.A. Gamage, R. Glover, Critical review of scintillating crystals for neutron detection, Crystals 9 (2019) 480.
[11] N. Kawano, T. Kato, G. Okada, N. Kawaguchi, T. Yanagida, Photoluminescence, scintillation and TSL properties of Eu-doped Al_2O_3 transparent ceramics synthesized by spark plasma sintering method, Opt. Mater. 88 (2019) 67–73.
[12] N. Wantana, E. Kaewnuam, Y. Ruangtaweep, P. Kidkhunthod, H.J. Kim, S. Kothan, J. Kaewkhao, High density tungsten gadolinium borate glasses doped with Eu^{3+} ion for photonic and scintillator applications, Radiat. Phys. Chem. 172 (2020), 108868.
[13] N. Kawano, M. Koshimizu, G. Okada, Y. Fujimoto, N. Kawaguchi, T. Yanagida, K. Asai, Scintillating organic–inorganic layered perovskite-type compounds and the gamma-ray detection capabilities, Sci. Rep. 7 (2017), 14754.
[14] R.E. Muenchausen, E.A. McKigney, L.G. Jacobsohn, M.W. Blair, B.L. Bennett, D. W. Cooke, Science and application of oxyorthosilicate nanophosphors, IEEE Trans. Nucl. Sci. 55 (2008) 1532–1535.
[15] L.G. Jacobsohn, K.B. Sprinkle, C.J. Kucera, T.L. James, S.A. Roberts, H. Qian, E. G. Yukihara, T.A. DeVol, J. Ballato, Synthesis, luminescence and scintillation of

rare earth doped lanthanum fluoride nanoparticles, Opt. Mater. 33 (2010) 136–140.
[16] I.J. Tillman, M.A. Dettman, V.V. Herrig, Z.L. Thune, A.J. Zieser, S.F. Michalek, M. O. Been, M.M. Martinez-Szewczyk, H.J. Koster, C.J. Wilkinson, M.W. Kielty, L. G. Jacobsohn, U. Akgun, High-density scintillating glasses for a proton imaging detector, Opt. Mater. 68 (2017) 58–62.
[17] S.F. Wang, J. Zhang, D.W. Luo, F. Gua, D.Y. Tang, Z.L. Dong, G.E.B. Tan, W.X. Que, T.S. Zhang, S. Li, L.B. Kong, Transparent ceramics: processing, materials and applications, Prog. Solid State Chem. 41 (2013) 20–54.
[18] A.A. Trofimov, L.G. Jacobsohn, Radioluminescence of $Lu_3Al_5O_{12}$:Ce single crystal and transparent polycrystalline ceramic at high temperatures, Ceram. Int. 46 (2020) 26335–26338.
[19] M.G. Chapman, M.R. Marchewka, S.A. Roberts, J.M. Schmitt, C. McMillen, C. J. Kucera, T.A. DeVol, J. Ballato, L.G. Jacobsohn, Luminescence and scintillation enhancement of Y_2O_3:Tm transparent ceramic through post-fabrication thermal processing, J. Lumin. 165 (2015) 56–61.
[20] T. Kunikata, T. Kato, D. Shiratori, D. Nakauchi, N. Kawaguchi, T. Yanagida, Scintillation properties of Li-doped ZnO translucent ceramics, Sensor. Mater. 34 (2022) 661–668.
[21] H. Kimura, T. Kato, D. Nakauchi, N. Kawaguchi, T. Yanagida, Optical, TSL and OSL properties of copper-doped cesium bromide transparent ceramics prepared by SPS, Sensor. Mater. 33 (2021) 2187–2193.
[22] A.A. Trofimov, J.C.A. Santos, D.V. Sampaio, R.S. Silva, T.A. DeVol, L.G. Jacobsohn, Microstructure, luminescence and thermoluminescence of laser-sintered polycrystalline ceramic YAG:Ce scintillators, J. Lumin. 251 (2022), 119206.
[23] N.R.S. Souza, D.C. Silva, D.V. Sampaio, M.V.S. Rezende, C. Kucera, A.A. Trofimov, L.G. Jacobsohn, J. Ballato, R.S. Silva, Laser sintering of persistent luminescent $CaAl_2O_4:Eu^{2+}Dy^{3+}$ ceramics, Opt. Mater. 68 (2017) 2–6.
[24] L.G. Jacobsohn, K. Serivalsatit, C.A. Quarles, J. Ballato, Investigation of Er-doped Sc_2O_3 transparent ceramics by positron annihilation spectroscopy, J. Mater. Sci. 50 (2015) 3183–3188.
[25] P.Y. Poma, K. Upendra Kumar, M.V.D. Vermelho, K. Serivalsatit, S.A. Roberts, C. J. Kucera, J. Ballato, L.G. Jacobsohn, C. Jacinto, Luminescence and thermal lensing characterization of singly Eu^{3+} and Tm^{3+} doped Y_2O_3 transparent ceramics, J. Lumin. 161 (2015) 306–312.
[26] N.J. Cherepy, J.D. Kuntz, Z.M. Seeley, S.E. Fisher, O.B. Drury, B.W. Sturm, T. A. Hurst, R.D. Sanner, J.J. Roberts, S.A. Payne, Transparent ceramic scintillators for gamma spectroscopy and radiography, 78050I-1-5, Proc. SPIE 7805 (2010).
[27] A. Ikesue, Ce:YAG ceramic scintillator for electron beam detector, J. Ceram. Soc. Jpn. 108 (2000) 1020–1023.
[28] W. Xie, J. Wang, M. Cao, Z. Hu, Y. Feng, X. Chen, N. Jiang, J. Dai, Y. Shi, V. Babin, E. Mihokova, M. Nikl, J. Li, Fabrication and properties of Eu:Lu_2O_3 transparent ceramics for X-ray radiation detectors, Opt. Mater. 80 (2018) 22–29.
[29] N.J. Cherepy, J.D. Kuntz, T.M. Tillotson, D.T. Speaks, S.A. Payne, B.H.T. Chai, Y. P-Chapman, S.E. Derenzo, Cerium-doped single crystal and transparent ceramic lutetium aluminum garnet scintillators, Nucl. Instrum. Methods Phys. Res., Sect. A 579 (2007) 38–41.
[30] F. Nakamura, T. Kato, G. Okada, N. Kawaguchi, K. Fukuda, T. Yanagida, Scintillation and dosimeter properties of CaF_2 transparent ceramic doped with Eu^{2+}, Ceram. Int. 43 (2017) 604–609.
[31] F. Nakamura, T. Kato, G. Okada, N. Kawaguchi, K. Fukuda, T. Yanagida, Scintillation and dosimeter properties of CaF_2 translucent ceramic produced by SPS, J. Eur. Ceram. Soc. 37 (2017) 1707–1711.
[32] T. Kato, N. Kawano, G. Okada, N. Kawaguchi, K. Fukuda, T. Yanagida, Scintillation properties of SrF_2 translucent ceramics and crystal, Optik 168 (2018) 956–962.
[33] F. Nakamura, T. Kato, G. Okada, N. Kawaguchi, K. Fukuda, T. Yanagida, Scintillation, TSL and RPL properties of MgF_2 transparent ceramic and single crystal, Ceram. Int. 43 (2017) 7211–7215.
[34] L.G. Jacobsohn, A.L. Roy, C.L. McPherson, C.J. Kucera, L.C. Oliveira, E. G. Yukihara, J. Ballato, Rare earth-doped nanocrystalline MgF_2: synthesis, luminescence and thermoluminescence, Opt. Mater. 35 (2013) 2461–2464.
[35] T. Kato, G. Okada, K. Fukuda, T. Yanagida, Development of BaF_2 transparent ceramics and evaluation of the scintillation properties, Radiat. Meas. 106 (2017) 140–146.
[36] L.G. Jacobsohn, C.L. McPherson, K.B. Sprinkle, E.G. Yukihara, T.A. DeVol, J. Ballato, Scintillation of rare earth doped fluoride nanoparticles, Appl. Phys. Lett. 99 (2011), 113111.
[37] R. Visser, P. Dorenbos, C.W.E. van Eijk, R.W. Hollander, P. Schotanus, Scintillation properties of Ce^{3+} doped BaF_2 crystals, IEEE Trans. Nucl. Sci. 38 (1991) 178–183.
[38] J. Luo, S. Sahi, M. Groza, Z. Wang, L. Ma, W. Chen, A. Burger, R. Kenarangui, T. K. Sham, F.A. Selim, Luminescence and scintillation properties of BaF_2–Ce transparent ceramic, Opt. Mater. 58 (2016) 353.
[39] N. Kawano, T. Kato, G. Okada, N. Kawaguchi, T. Yanagida, Optical, scintillation and dosimeter properties of MgO:Tb translucent ceramics synthesized by the SPS method, Opt. Mater. 73 (2017) 364.
[40] T.A. Lodi, J.F.M. dos Santos, G. Galleani, L.G. Jacobsohn, T. Catunda, A.S.S. de Camargo, Promising Tb^{3+}-doped gallium tungsten-phosphate glass scintillator: spectroscopy, energy transfer, and UV/X-ray sensing, J. Alloys Compd. 904 (2022), 164016.
[41] J.C.A. Santos, E.P. Silva, N.R.S. Souza, Y.G.S. Alves, D.V. Sampaio, C. Kucera, L. G. Jacobsohn, J. Ballato, R.S. Silva, Laser sintering and photoluminescence study of Tb-doped yttrium aluminum garnet ceramics, Ceram. Int. 45 (2019) 3797–3802.
[42] T. Yanagida, G. Okada, N. Kawauchi, Ionizing-radiation-induced storage-luminescence for dosimetric applications, J. Lumin. 207 (2019) 14–21.
[43] P. Leblans, D. Vandenbroucke, P. Willems, Storage phosphors for medical imaging, Materials 4 (2011) 1034–1086.
[44] K. Shinsho, Y. Kawaji, S. Yanagisawa, K. Otsubo, Y. Koba, G. Wakabayashi, K. Matsumoto, H. Ushiba, X-ray imaging using the thermoluminescent properties of commercial Al_2O_3 ceramic plates, Appl. Radiat. Isot. 111 (2016) 117–123.
[45] T. Yanagida, K. Kamada, Y. Fujimoto, H. Yagi, T. Yanagitani, Comparative study of ceramic and single crystal Ce:GAGG scintillator, Opt. Mater. 35 (2013) 2480–2485.
[46] T. Yanagida, Y. Fujimoto, T. Ito, K. Uchiyama, K. Mori, Development of X-ray-induced afterglow characterization system, APEX 7 (2014), 062401.
[47] N. Kawano, D. Nakauchi, F. Nakaumura, T. Yanagida, Scintillation and dosimetric properties of Tb-doped CaF_2 translucent ceramics synthesized by the spark plasma sintering method, J. Asia. Ceram. Soc. 8 (2) (2020) 484–491.
[48] N. Kawano, M. Akatsuka, H. Kimura, G. Okada, N. Kawaguchi, T. Yanagida, Scintillation and TSL properties of Tb-doped $NaPO_3$-$Al(PO_3)_3$ glasses, Radiat. Meas. 117 (2018) 52–56.
[49] R.E. Muenchausen, L.G. Jacobsohn, B.L. Bennett, E.A. McKigney, J.F. Smith, J. A. Valdez, D.W. Cooke, Effects of Tb doping on the photoluminescence of Y_2O_3:Tb nanophosphors, J. Lumin. 126 (2007) 838–842.
[50] N. Kawano, H. Kimura, M. Akatsuka, D. Nakauchi, G. Okada, T. Yanagida, Scintillation and thermoluminescent properties of Dy-doped calcium borate chloride, Opt. Mater. 112 (2021), 110784.
[51] L. Pan, S. Sholom, S.W.S. McKeever, L.G. Jacobsohn, Magnesium aluminate spinel for optically stimulated luminescence dosimetry, J. Alloys Compd. 880 (2021), 160503.
[52] H. Kimura, T. Kato, T. Fujiwara, M. Tanaka, G. Okada, D. Nakauchi, N. Kawaguchi, T. Yanagida, Optical and photostimulated luminescence properties of Eu:BaFBr translucent ceramics synthesized by SPS, Ceram. Int. 49 (2023) 15315–15319.